Int. J. Electrochem. Sci., 13 **(2018)** 6779 – 6790, doi: 10.20964/2018.07.10

International Journal of
ELECTROCHEMICAL
SCIENCE
www.electrochemsci.org

Corrosion Behaviors of Copper Exposed to an Urban Atmosphere

Ye Wan[*]*, Haixiao Zhang, Yanbo Li, Xiumei Wang, Fan Zhaorong, Xu Zhu*

School of Materials Science and Engineering, Shenyang Jianzhu University, Shenyang 110168, China
[*]E-mail: ywan@sjzu.edu.cn

Received: 27 February 2018 / *Accepted:* 21 April 2018 / *Published:* 5 June 2018

Copper was exposed for a total period of six months in an urban atmosphere, Shenyang site of China. The corrosion data of the exposed copper were collected for monthly intervals. The products and the corrosion amounts accumulated on the exposed copper have been investigated by mass loss, scanning electron microscopy, X-ray diffraction and coulometric reduction. The corrosion loss calculated from the reduction charges were compared with mass loss from the weight technique. The primary corrosion products found on field-exposed samples were copper oxides. For shorter exposure, such as no more than one month, the corrosion products were composed of Cu_2O and CuO. For more than two month exposure, the chemical components were mainly Cu_2O and CuO, and $Cu_2(OH)_3Cl$ and Cu_2S were also observed on the surface of the field exposed copper. The corrosion mechnisms of copper at Shenyang site are proposed as well.

Keywords: Copper; Atmospheric corrosion; Field exposure; Copper oxides; Coulomtric reduction

1. INTRODUCTION

As an important functional material, copper has attracted a great amount of interest owing to its significant technological properties. It has been widely used in versatile engineering structures, such as heat exchangers in chemical engineering, conductive material in electrical and information engineering, roofs and claddings in external constructions on the basis of its promising electronic, thermal, mechanical and chemical properties. Generally, copper is safe to be used for its good corrosion resistance in the dry atmospheres. However, patina appears on the surface of copper owing to atmospheric corrosion in the wet atmospheres.

Atmospheric corrosion, essentially a result of several physicochemical reactions between materials and their surround environments [1], has long been confirmed to cause significant damage. Because of the rapid industrial growth, atmospheric pollution is a serious problem over the world

especially in Asia in recent years [2, 3]. The species including sulfur and chlorine in the atmospheres are typical factors in the atmospheric corrosion of copper. Sodium chloride in sea-salt aerosols and hydrogen chloride emitted from incineration plants are mainly chlorine-containing species [4]. Hydrogen sulfide from hot springs and sulfur dioxide from fossil fuel combustion are typical sulfur-containing gases [4]. During the outdoor exposure, the existence of the chemical contaminants in the atmosphere, such as the chlorine-containing species and the sulfur-containing gases, promote corrosion of copper [4, 5]. The typical chloride-containing salts and sulfur-containing gases were deposited or adsorbed on the surface of copper exposed in the atmospheres. Due to hygroscopic nature of the species, they deposit on the copper surface and absorb water from the atmospheres, and then a thin electrolyte is formed. The electrochemical micro-cells formed due to the ions in the electrolyte on the surface facilitate copper corrosion.

It is known that indoor atmospheric corrosion obeys the same fundamental reactions as outdoors in most cases [6]. Many accelerated indoor testing techniques, such as salt spray tests, wet-dry cyclic accelerated testing, have been used to investigate the corrosion behavior. However, at actual environmental conditions, the variations in relative humidity, temperature, UV light and the polluting species are intricate, and it is hard to recognize the real corrosion behaviors of copper by using indoor exposure. The field exposure provides actual information on the atmospheric corrosion behaviors of materials, and it is the most important method to investigate atmospheric corrosion [6]. Many field tests were carried out to check the corrosion behaviors for the safety application of materials in various atmospheric environments [7-11].

The goal of this study was to extend the previous work by exposing copper in an actual atmosphere. Shenyang, also known as Fengtian and located at the center of the Northeast Asia Economic Circle and the Bohai Rim Economic Circle, is the only mega-city around the Bohai Sea and Northeast China. Shenyang is the important central city, the advanced equipment manufacturing base and the national historical and cultural city in Northeast China. For Shenyang's long-term development, it is very important to investigate its atmosphere and the durability of materials in this area. Therefore, Shenyang, an urban atmosphere, was chosen to be a field exposure site to understand the corrosion mechanism and corrosion rates of copper. Many methods, such as weight measurement, X-ray diffraction, scanning electron microscopy, couloumetric reduction, were used to identify the corrosion products and the corrosion amounts of the exposed copper in the field site.

2. EXPERIMENTAL

Sample preparation.− All copper coupons were 99.99% pure and 40 *mm* × 20 *mm* × 3 *mm* in size. They were ground sequentially with 800 and 1000 grit SiC paper, followed by 1.5 μm diamond polishing, degreased with alcohol and rinsed with deionized (DI) water, dried and stored in a desiccator with silica gel for at least 24 hours before exposure. High purity deionized water (Millipore > 20 MΩ cm) was used throughout.

Field exposure.− The copper coupons were exposed at the geolocation of Liaoning province in China: Shenyang, a temperate semi-humid continental climate. The exposure began in May and lasted

for up to six months and one month was an exposure cycle. The exposure method was described in detail elsewhere [12]. The field site is in the northeast of China, and the environmental factors, such as UV light intensity, O_3 concentration, relative humidity and temperature, in Shenyang site increase from May to August and decrease in the following two months. The Average environmental parameters at the field site through May to October are listed in Table 1. An ultraviolet (UV) power meter (Model FU-100†, Skyworth Science and Technology Development Co., Ltd., Beijing, China) was used to measure the UV light intensity of the atmosphere. The concentration of ozone was recorded with an ozone analyzer (WT-80, Weitai Science & Technology Co., Ltd., Shanghai, China) generally used for monitoring ambient air. Relative humidity (RH) was monitored with an AZ8708 RH meter (Hengxin, Chinese Taipei).

Table 1. Average environmental parameters at Shenyang Site through May to October

Average UV light intensity, W/m^2	Average O_3 concentration, ppb	Average relative humidity (RH), %	Average temperature, ºC
18.8	50.2	56.3	10-25

Details of the electrochemical method.− After exposure, some of the coupons were conducted with a conventional three-electrode cell to quantify the amount of corrosion products with the coulometric reduction technique, which was described in detail in the previous work [13]. The reduction potential and the reduction charge were extracted from each reduction curve. The thickness of the corrosion product layer of copper was calculated from the reduction charge, assuming that the corrosion product film forms with a theoretical density. The cell exposed 1 cm^2 portions of the coupons to be work electrodes. A flat platinum mesh was served as the counter electrode. All the potentials were measured against an Hg/Hg_2Cl_2/saturated KCl reference electrode (SCE, + 0.244 V/NHE). The electrochemical experiments were conducted with an electrochemical instrument (LK3200A, Lanlike Co. Ltd., Tianjin, CN) combined with an electrochemistry software named LK3200A®. A constant reduction current density of -1 mA/cm^2 was used for the coulometric reduction. 0.1 M KCl was served as the supporting electrolyte for coulometric reduction test [14, 15]. According to the recommendation of ASTM B825 [14], 0.1 $mol \cdot L^{-1}$ potassium chloride (KCl) solution (pH=10) was used for the coulometric reduction electrolyte where copper oxides were mainly the expected corrosion products. The preparation of the electrolyte and the procedure of the coulometric reduction were described in detail in the previous work [16]. KCl solution was made from Sinopharm certified KCl and deionized water. The electrolyte for cyclic voltammetry (CV) was 0.1 $mol \cdot L^{-1}$ potassium hydroxide, KOH.

Mass loss.− In order to determine the corrosion rates of the copper coupons for different exposure duration, mass of the coupons was recorded before exposure and after being cleaned. The following procedure for the removal of corrosion products on the coupons was performed at the ambient temperature. The coupons were first rinsed by a flux of deionized water to remove water-soluble corrosion products, and then immersed 5 minutes in the rust removing solution to remove the

remainder of the corrosion products. The chemical cleaning procedures accorded to Reference 17 as follows. The rust removing solution, 10% (wt.) H_2SO_4, was prepared by mixing 100 mL sulfuric acid (H_2SO_4, sp gr 1.84g/mL) with deionized water to be 1000 mL solution. Afterwards, the coupons were cleaned by deionized water to remove the residual ions from the rust removing solution. They were repeated for another 5 minute soaking in the rust removing solution. The copper coupons are cleaned a max of 10 minutes, two 5-minute cycles. Then the coupons were finally rinsed with deionized water and anhydrous alcohol, dried with nitrogen gas and recorded the mass. The mass loss was determined after each cleaning by weighing the specimen before and after cleaning. The mass loss during the rust removal was corrected with the unexposed coupons.

Characterization.− After retrieved from the exposure site, the surface chemistry of the copper coupons was examined with many methods. The morphologies of the copper coupons were checked using scanning electron microscopy (FEI Verrios 400, FEI, Netherlands) at 15 kV. The compositional analysis was determined by energy dispersive X-ray spectroscopy (EDX) on the S-4800 FE-SEM. X-ray diffraction (XRD) measurements were taken on a D/MAX 2400 instrument (Rigaku) with a RINT 2000 wide-angle goniometer and Cu $K\alpha_1$ radiation (λ = 1.54056 Å) to identify the specimen's structures. The diffraction patterns were scanned over an angular (2θ) range of 20°-90° at intervals of 0.04°. Resulting diffraction patterns were analyzed and peaks were identified using Jade® Software (version 6.5, Material Data Inc., California, USA). All the measurements were taken at room temperature unless otherwise specified.

3. RESULT

3.1 Mass loss

Cumulative corrosion quantity of the copper coupon was expressed as mass loss after coupon cleaning through the end of each time period. Figure 1 shows the mass loss as a function of exposure time for the coupons exposed at Shenyang Site. The black square icons in Figure 1 are the average mass loss data. It is clearly seen from Figure 1 that the mass loss increases with the exposure time going on. The mass loss grew nearly linear during the first four months from May to August. Then the growth rate slowed down a little bit during the following two months. After exposed in the atmosphere, the corrosion compounds were formed on the surface of the bulk copper and should retard the corrosion rate. It is well known that the reaction rate increases with temperature. The initial linear metal loss didn't slow down is possibly because the atmosphere became hotter and wetter from May to August. Conversely, the temperature of air decreases slowly after September and reduces corrosion rate of copper. The reciprocal effects of corrosion products and environmental temperature draw mass loss of approximate initial linear growth followed by a down-bending growth.

The error bars, based on standard deviation, of the mass loss of the coupons for every cycle in red are shown in Fig.1 as well. The error bars shown for each data point of Fig. 1 are the distribution of mass loss measurements during every exposure cycles. Note that the separation between upper and lower mass losses is greater than 40 indicating that the mass loss vary over a large range about 10% of

the mass loss. The error bars depicts the standard deviation was the largest in the first exposure cycle and decreased a little bit for the following exposure.

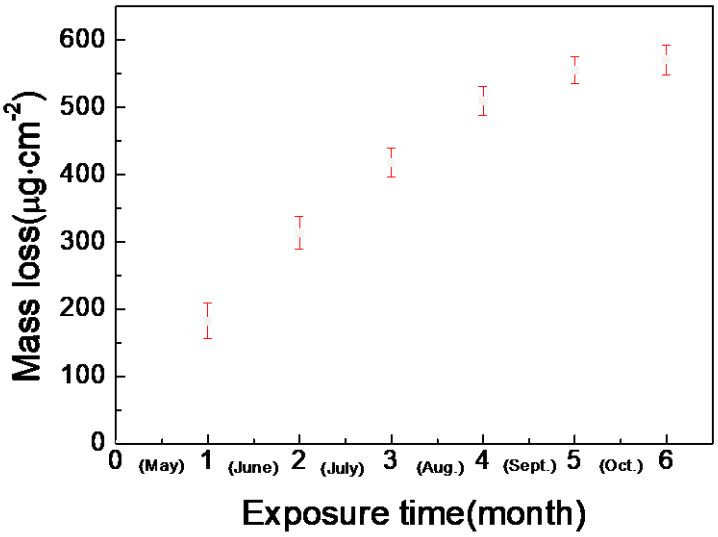

Figure 1. Mass loss and the error bars of copper with the exposure time at Shenyang site. (Error bar: one standard deviation) Error bars show the distribution of mass losses of the coupons during the exposure cycles.

3.2 SEM morphology

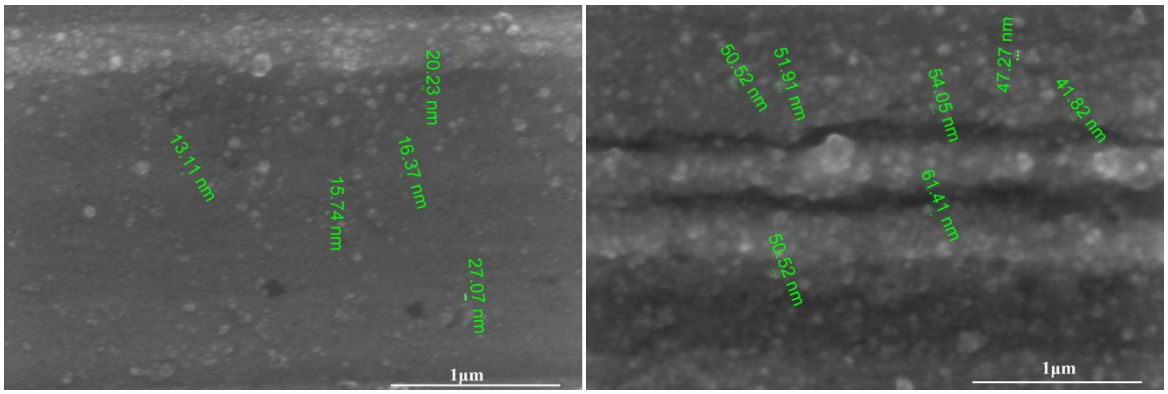

(a) (b)

Figure 2. Surface SEM images of the copper coupons after exposure at Shenyang site for (a) three months and (b) six months.

Figure 2 (a) and (b) depict the SEM morphologies of the copper coupons after exposed for three and six months at Shenyang site respectively. It can be seen that the surface image of the coupon exposed for six months is similar to that with a three-month exposure. The corrosion products formed on the surfaces display a granular nature for the coupons whether exposed for three or six months. The particles of the corrosion products unevenly distribute over the sample. The coupons with a six-month

exposure corroded more severely than that of the coupon with a three-month exposure. The particle diameter of the corrosion products is about 50 nm for the coupons with a six-month exposure, while it is approximate 15 nm for the coupons after exposed for three months. SEM observations also show that corrosion proceeds seriously at the internal defects of copper. For instance, at the polishing groove, the corrosion products along the grinding stripe are bigger and thicker than that in the plat areas on the surface of the six-month exposure coupon, seen in Figure 2(b).

3.3 Structure identification of corrosion compounds by XRD

In order to identify the corrosion compounds, the XRD patterns of the copper coupons after exposed for one month and two months at the field site were recorded and are shown in Fig. 3. It is revealed that the diffraction peaks of Fig. 3(a) agree well with those recorded on JCPDS cards 85-1326 (Cu), 74-1230 (Cu_2O) and 80-1987 (CuO). The relative intensities of Cu_2O is much higher than that of CuO, seen in Fig. 3(a).

Comparing the diffraction peaks of Fig. 3(a) and 3(b), it is clear that an increase of the exposure time resulted in many new broad and weak diffraciton peaks, which indicates that new compounds were formed. For example, on the basis of the XRD pattern of the copper coupon exposed for two months at the field site in Fig. 3(b), it can be drawn that the corrosion products are mainly Cu, Cu_2O and CuO, and the weak diffraction peaks of $Cu_2(OH)_3Cl$ and Cu_2S are manifested as well.

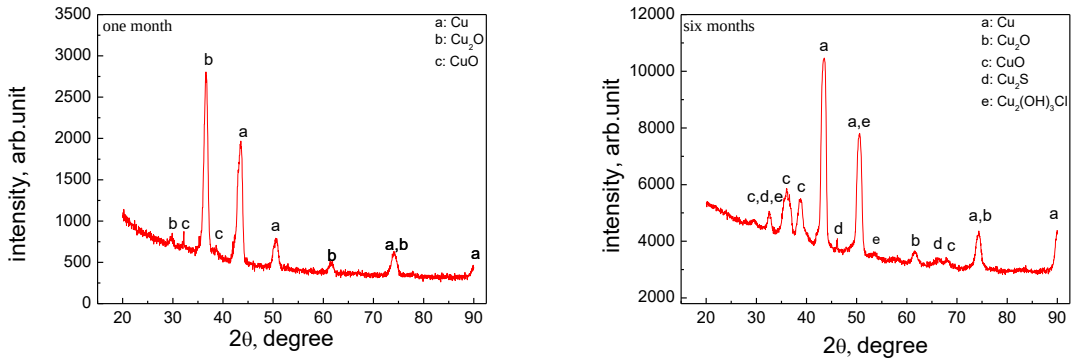

(a) (b)

Figure 3. XRD patterns of the Cu coupons exposed at the field site for one month (a) and two months (b).

3.4 Cyclic voltammetric curve

Cyclic voltammetric tests for a copper electrode were carried out in 0.1 $mol \cdot L^{-1}$ KOH solution with a scan rate of 40 $mV \cdot s^{-1}$ to identify redox processes which are determined by the significant potential regions, during the formation and reduction of the copper oxides in Fig. 4.

The peaks labeled A1 (located at ca. -0.47 V) and A2 (located at ca. -0.01 V) correspond to the formation of Cu_2O and CuO respectively on the positive-going scan. There is a pre-peak at approximately -0.17 V might belong to a monolayer of CuO as a precursor to the formation of a bulk

film of the phase CuO through the relation procedure from Cu_2O and CuO. The two cathodic peaks, labeled C_1 (- 0.98 V) and C_2 (- 0.62 V), arise during the reverse scan and are complementary to the reduction potential positions of Peak A1 and Peak A2. Peak C_2 and Peak C_1 are due to the electro-reductions from CuO to Cu_2O and Cu_2O to native copper, which agrees with Lenglet's assignment that the first peak (C1) on the voltammogram to the reduction of Cu_2O and the second peak (C2) to the reduction of CuO [18].

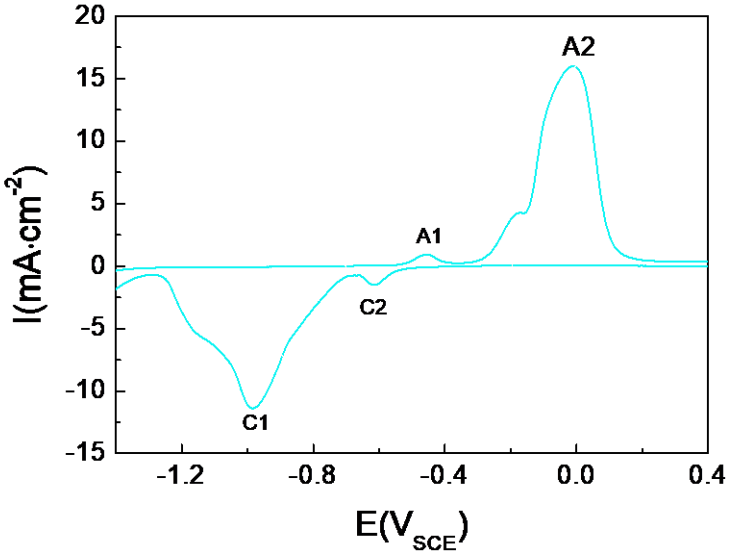

Figure 4. Cyclic voltammograms of copper in 0.1 mol·L^{-1} KOH at 40 mV/s scan rate.

3.5 Phase identification of corrosion compounds by electrochemical tests

The corrosion amounts of copper exposed for three months at the field site are evaluated via the coulometric reduction method. Coulometric reduction is an electrolytic method that measures the potential as a function of reduction time and is used to identify both the compound and determine the amount presented. The potential plateau position of the coulometric reduction curve can be used to identify the compound and the time during which the plateau is maintained can be related to the amount of corrosion product via Faraday's Second Law[13]. A typical coulometric reduction curve of the copper coupons after exposed three months at the field site is shown in Fig. 5. During the reduction performation of the coupon in Fig. 5, there are three distinct stages according to the reduction potentials and plateaus: at about - 0.67 V (Stage 1, named S1), at aobut -0.97 V (Stage 2, named S2) and at approximately -1.4 V (Stage 3, named S3). Based on the results of the cyclic voltammetry from Fig. 4, the first plateau at -0.67 V belongs to the reduction potentials of CuO to Cu_2O. The second plateau, at approximately -0.97 V, corresponds to the reduction potential of Cu_2O to native copper. At the third stage, the potential drops sharply to approximately -1.4 V, which indicates that the copper oxides are deoxidized totally and hydrogen evolution occurs.

The reduction time is defined as from the beginning to the midpoint between the adjacent two plateaus [13]. Fig. 5 depicts the reduction time for the corrosion compounds of copper after exposure

at Shenyang site. The reduction time for Cu_2O is the time of the green stage maked by S1 from the beginning to the first dashed lines, while the CuO is the time of the blue stage maked by S2 between the first and the second dashed lines. The reduction time are extracted from the coulometric reduction curves. The corresponding reduction charges are calculated from the reduction time via multiplying by the current density, which is constant (-1 mA/cm^2) in this work.

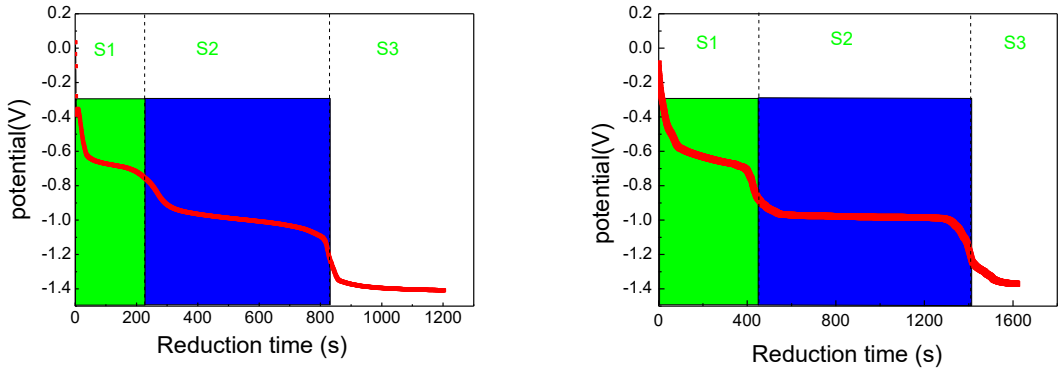

Figure 5. Coulometric reduction curves of the copper coupons after exposed for three months (a) and six months (b) at the field site. Note: the reduction current is -1 mA/cm^2 and the electrolyte is 0.1 mol/L KCl (pH=10).

The chemical identity of the reducible component is mainly inferred as the copper oxides. The total mass of all the components of the entire film can be obtained by adding the respective values for these known or inferred constituents [19]. Assuming that it is present as an homogeneous layer in the oxides film, for the mass of a known substance, the mass of the substance reduced by the coulometric reduction methods is calculated according to Eq. (1) on the basis of Reference 14 and Reference 19.

$$W = it\frac{10^3 M}{NF} \quad (1)$$

where:

W = mass, μg,

i = current, mA,

t = time, s, to reduce a known substance, copper,

M = gram-molecular weight of that substance copper,

F = Faraday's constant (9.65×10^4 C), and

N = number of faradays required to reduce a grammolecular weight of the substance, 2 for Cu_2O and CuO.

Corrosion amounts, expressed as reduction time, reducation charges and mass loss, of copper after exposed three months and six months at Shenyang site are calculated accoding to Fig. 5. The results are depicted in Table 2. It can be seen from Table 2 that the amount of Cu_2O is approximate one third of CuO for both of the exposures. The total reduction time for three-month exposure is nearly half of that for six-month exposure.

Table 2. Corrosion amounts of copper after exposed at Shenyang site.

Exposed time, month	RT[a] of Cu_2O, s	RT of CuO, s	Total RT, s	Total RC[b], mC/cm^2	Mass loss, $\mu g/cm^2$
3	200	606	806	80.6	265
6	385	1001	1386	138.6	456

a: RT refers to reduction time. b: RC refers to reduction charge.

4. DISCUSSION

It is known that copper is resistant to corrosive attack in the normal unpolluted dry environments, but it is quite vulnerable to the pollutants present in the atmospheres [20]. The mass loss has been determined by weight technique for the exposed copper at Shenyang site, illustrated in Fig. 1. The mass loss calculated from the coulometric reduction charges is shown in Table 2. The mass loss by the weight technique are $417.7\mu g/cm^2$ and $570.4\mu g/cm^2$ respectively for the three-month exposure and the six-month exposure. Assuming that the average corrosion rate of copper is the same during the whole year, annual corrosion rates for the mass losses of $417.7\mu g/cm^2$ (three months) and $570.4\mu g/cm^2$ (six months) were converted to be $16.7 g\cdot m^{-2}\cdot y^{-1}$ and $11.4 g\cdot m^{-2}\cdot y^{-1}$ respectively. Comparing the annual corrosion rates of copper at different field site, it is drawn that the corrosion rate of copper at Shenyang is close to that at St. Anne [21]. It is important to note that reduced average corrosion rates with time persisted during the whole exposure period, seen from the mass loss in Fig. 1.

The calculated mass loss from the coulometric reduction is $265.2\mu g/cm^2$ and $456\mu g/cm^2$ respectively for the three-month exposure and the six-month exposure. It can be seen that the mass loss via the weight technique is about 1.5 times of the mass loss by the coulometric reduciton method. One reason for the difference of the mass loss between the two methods is possibly because the oxides film is exactly not a homogeneous layer, which is mainly made up of Cu_2O and CuO. The other reason is because the chemical composition in the film includes unreducible $Cu_2(OH)_3Cl$, seen in Fig. 3(b). The unreducible compounds weren't detected via the coulometric reduction method and made a pseudo-decrease in the corrosion amounts. However, for the coulometric reduction and the weight technique, the corrosion amounts have similar ratios of the three-month exposure' data to the six-month exposure' data. Moreover, the coulometric technique can also be used to determine the relative proportions of the different reducible corrosion products making up the overall tarnish film, while the weight loss technique can't.

Observed differences in mass loss are attributed to changes in the outermost patina composition and characteristics with time [21]. In this work, the XRD patterns and the coulometric reduction have assessed the corrosion compounds of copper and the main compounds are found to be copper oxides on the coupons from Shenyang site. After the first month exposure, the corrosion compounds are mainly made of CuO and Cu_2O. It is surprised that no chloride or sulfur formation appears as would be expected during the field exposure. It is believed that the peaks of the corrosion products in the XRD patterns evolve with exposure time. During the first month expsoure at Shenyang site in May, the atmosphere is dry, and atmospheric corrosion is expected to initiate on copper surface as a result of

oxygen attack in the field exposure. Based on the XRD data (Fig. 3) of the coupons exposed for one month (throughout May), the copper oxides are formed on the copper surfaces, which is in agreement with the expection. The domain corrosion compounds of the coupons after a two month exposure at the field site are basically CuO and Cu_2O, which were recorded by XRD and the coulometric techniques. However, the diffraction peaks of $Cu_2(OH)_3Cl$ and Cu_2S appear after the two-month exposure, which suggests that $Cu_2(OH)_3Cl$ and Cu_2S were formed for a longer exposure than one month.

XRD of copper exposed for two months reveals $Cu_2(OH)_3Cl$ to be a minor corrosion product, seen in Fig. 3. This phenomenon agrees with Lin and Skennerton's reports that the copper products involved in $Cu_2(OH)_3Cl$, which usually appears after several months of marine exposure [22, 23]. Shenyang represents a city environment and not far away from the Bohai Sea, which contributes to NaCl deposition on the surfaces of copper. Note that the patina on copper was composed of two main layers, Cu_2O as the inner layer and $Cu_2(OH)_3Cl$ as the outer layer [24]. The characteristics of the corrosion products formed on the copper surface affects its long-term corrosion rate. It is known that specimens with higher roughness values exhibited more corrosion when compared to smoother specimens when exposed to a corrosive environment for same duration [21], and the big particles results in a rougher surface. The particles of the corrosion products after a six-month exposure is quilt larger than that with a three month exposure (Fig. 2), which gives an evidence to the hypothesis of increased corrosion loss with exposure time. The formed corrosion particles occupy the copper surface and act as a passivation layer to retard a further fast corrosion of copper in the atmosphere. During the three months from July to September, RH of the atmosphere increases and a thicker layer of electrolyte appears on the copper surface. Deposit of the contamination, such as chloride compounds and sulfur compounds, in the layer increases the corrosion drive force of copper and makes a liner increase of mass loss during the first four month exposure (Fig. 1). The other reason for the initial linear growth is attributed to a higher initial surface roughness of the coupons as well. From September, the corrosion rate decreases because of the passivation-like layer of the corrosion products and temperature drop of the surrounding atmosphere.

A thin protective layer of Cu_2O and CuO develops on the copper surface of in the non-polluted atmospheres. However, the diverse pollutants in the city atmosphere (Shenyang, 150Km from the coastal line) such as the chlorine-containing species and the sulfur-containing gases breach the protective oxide film formed on the metal surface. The results of XRD show the lightly presence of $Cu_2(OH)_3Cl$ compound on the surface of the copper coupon after exposure at the field site, which agrees well with the results of the copper coupon after the laboratory exposure by Lin et al.[21]. Although the weak diffraction peak of $Cu_2(OH)_3Cl$ and Cu_2S are observed in Fig. 3 for the outdoor site, the copper oxides are the main dominant corrosion products. It is also believed from the corrosion products containing Cl and S elements that there are a little chloride contamination and sulfur contamination deposited on the surface of the coupons after a two-month exposure at the field site. Comparatively, there is not enough chloride and sulfur deposit to build detectable $Cu_2(OH)_3Cl$ and Cu_2S on the surface of the coupons after an one-month exposure. The XRD analysis confirms deposit of chloride and sulfur contamintaion on the coupons at the field site and the contamintaion accumulation depends on the exposure time as well. The results of the compound changes is not only

related to the exposure time, but also an evidence of chloride and sulfur contamination present in low concentrations in the urban atmosphere.

The chloride contamination chemicals, depositing on the surface of th exposoed copper, form $Cu_2(OH)_3Cl$ with the initial copper oxides in the atmosphere [21, 25]. The formation of $Cu_2(OH)_3Cl$ is shown in Eq.(2).

$$2Cu_2O + O_2 + 2Cl^- + 4H_2O \rightarrow 2Cu_2(OH)_3Cl + 2OH^- \quad (2)$$

5. CONCLUSIONS

Field exposure was conducted in Shenyang, a temperate semi-humid continental climate, to investigate the real corrosion behaviors of copper. Mass loss by weight technique follows an approximate initial linear growth followed by a down-bending growth with the exposure time. The mass loss via the weight technique is about 1.5 times of the mass loss by the coulometric reduction method. The corrosion amounts present similar ratios of the three-month exposure' data to the six-month exposure' data for both of the coulometric reduction and the weight technique. The particles of the corrosion products unevenly distributes over the sample. After a six-month exposure, the particle diameter of the corrosion products is bigger than that of the coupons after exposed for three months. The coupons with a six-month exposure corroded more severely than that of the coupon with a three month exposure. The main corrosion products are Cu_2O and CuO for one month exposure, while they are Cu_2O, CuO, $Cu_2(OH)_3Cl$ and Cu_2S for the copper exposed for two months.

ACKNOWLEDGMENTS

The authors gratefully appreciate the financial support from by Liaoning Natural Science Foundation (Grant No.: 2015020227) and Program for Changjiang Scholars and Innovative Research Team in University of Ministry of Education of China (Grant No.: IRT_15R45). Many thanks to Sucheng Wang at Institute of Metal Research, Chinese Academy of Sciences for XRD measurements.

References

1. S. Hosseinpour, M. Forslund, C.M. Johnson, J. Pan and C. Leygraf, *Surf. Sci*., 648 (2016) 170.
2. J.H. Tan, J.C. Duan, D.H. Chen, X.H. Wang, S.J. Guo, X.H. Bi, G.Y. Sheng, K.B. He and J.M. Fu, *Atmos. Res*., 94 (2009) 238.
3. P.D. Safai, S. Kewat, P.S. Praveen, P.S.P. Rao, G.A. Momin, K. Ali and P.C.S. Devara, *Atmos. Environ*., 41(2007) 2699.
4. M. Watanabe, E Toyoda, T Handa, T Ichino, N Kuwaki, Y. Higashi and T. Tanaka, *Corros. Sci*., 49 (2007) 766.
5. M. Watanabe, S. Shinozaki, E. Toyoda, K. Asakura, T. Ichino, N. Kuwaki, Y, Higashi and T. Tanaka, *Corros.*, 62 (2006) 243.
6. C. Pan, W.Y. Lv, Z.Y. Wang, W. Su, C. Wang and S.N. Liu, *J. Mater. Sci. Technol*., 33 (2017) 587.
7. L. Núñnez, E. Reguera, F. Corvo, E. González and C. Vazquez, *Corros. Sci*., 47 (2005) 461.
8. I.T.E. Fonseca, R. Picciochi, M.H. Mendonc and A.C. Ramos, *Corros. Sci*., 46 (2004) 547.
9. A.R. Mendoza and F. Corvo, *Corros. Sci*., 42 (2000) 1123.

10. S. Goidanich, J. Brunk, G. Herting, M.A. Arenas and I. O. Wallinder, *Sci. Total Environ.,* 412-413 (2011) 46.
11. G. Skennerton, J. Nairn and A. Atrens, *Mater. Lett*., 30 (1997) 141.
12. Y. Wan, X.L. Wang, X.M. Wang, Y.B. Li, H. Sun and Ke Zhang, *Int. J. Electrochem. Sci*., 10 (2015) 2336.
13. Y. Wan, E.N. Macha and R.G. Kelly, *Corros.*, 68 (2012) 036001-1.
14. ASTM, 'Standard test method for coulometric reduction of surface films on metallic test samples', in 'Annual book of ASTM standards', ASTM B825, ASTM, Philadelphia, PA, 2007.
15. H. Lin and G.S. Frankel, *J. Electrochem. Soc*., 160 (2013) C336.
16. Y. Wan, X. Wang, H. Sun, Y.B. Li, K. Zhang and Y.H. Wu, *Int. J. Electrochem. Sci*., 7 (2012) 7902.
17. ASTM, 'Standard practice for preparing, cleaning, and evaluating corrosion test specimens1', in 'Annual book of ASTM standards', ASTM G1-03, ASTM, Philadelphia, PA, 2003.
18. M. Lenglet, K. Kartouni and D. Delahaye, *J. Appl. Electrochem*., 21 (1991): 697-702.
19. A. Wolfenden, S.J. Krumbein, B. Newell and V. Pascucci, *J. Test. Eval*., 17 (1989) 357.
20. D. Saha, A. Pandya, J.K. Singh, S. Paswan, and D.D.N. Singh, *Atmos. Pollut. Res*., 7 (2016) 1037.
21. I.O. Wallinder, X. Zhang, S. Goidanichb, N.L. Bozec, G. Herting, and C. Leygraf, *Sci. Total. Environ.*, 472 (2014) 681.
22. H. Lin and G.S. Frankel, *Corros*., 48 (2013) 461.
23. G. Skennerton, J. Nairn, and A. Atrens, *Mater. Lett.,* 30 (1997) 141.
24. H.U. Sajid, and R. Kiran, *J. Constr. Steel. Res*., 144 (2018), 310.
25. H. Strandberg: *Atmos. Environ*., 32 (1998) 3521.